On multistep Bose-Einstein condensation in anisotropic traps

2000 J. Phys. A: Math. Gen. 33 487

(http://iopscience.iop.org/0305-4470/33/3/305)

J. Phys. A: Math. Gen. **33** (2000) 487–506. Printed in the UK PII: S0305-4470(00)05521-9

On multistep Bose–Einstein condensation in anisotropic traps

K Shiokawa

Department of Physics, University of Maryland, College Park, MD 20742, USA
and
Center for Nonlinear Studies, Hong Kong Baptist University, Kowloon Tong, Hong Kong
and
Theoretical Physics Institute, University of Alberta, Edmonton, Alberta, Canada T6G 2J1

E-mail: kshiok@phys.ualberta.ca

Received 25 June 1999, in final form 4 November 1999

Abstract. Multistep Bose–Einstein condensation of an ideal Bose gas in anisotropic harmonic atom traps is studied. In the presence of strong anisotropy realized by the different trap frequency in each direction, the finite size effect dictates a series of dimensional crossovers into lower-dimensional excitations. Two-step condensation and the dynamical reduction of the effective dimension can appear in three separate steps. When the multistep behaviour occurs, the occupation number of atoms excited in each dimension is shown to behave similarly as a function of the temperature. Multistep behaviours can be easily controlled by changing the degree of anisotropy.

1. Introduction

Although Bose–Einstein condensation (BEC) has been an active topic of research in condensed matter physics for decades [1–4], recent revival of interests in this field is mainly credited to the achievement in atom molecular optics; most recent laser cooling and evaporative cooling techniques in magnetic and optical atom traps enable us to realize BEC of a weakly interacting gas in a controlled way [5–7]. The weakly interacting nature of a gas allows us to handle the phenomena and make theoretical predictions with high accuracy. The rapid progress in this field also stimulates other areas in physics such as high-energy physics and astrophysics [8].

For atom trap experiments, since atoms are trapped in a finite geometry, finite size as well as finite number effects play a significant role in the condensation process. The conventional phase transition picture defined in the thermodynamic limit has to be re-examined or modified [9–16]. One significant change due to finiteness is the existence of BEC in low-dimensional systems. Recently, quasi-low-dimensional systems prepared by optical or magnetic trapping devices have been actively discussed [17, 18]. The study of such systems provides an ideal test for the theory of finite size, low-dimensional systems in a controlled environment.

The critical behaviour of a finite size system [19–21] is characterized by the effective infrared dimension (EIRD) of the system [22, 23]: near the critical point when the contribution of the lowest mode of a system dominates, its symmetry properties can be shown to be equivalent to a lower-dimensional one. The system, in such a case, is said to possess an EIRD. Varying the relative size (or shape) of the potential changes the infrared behaviour and hence the EIRD of the system.

Dimensionless parameters $\eta_i = \beta\hbar\omega_i$ ($\beta = 1/k_BT$) for a harmonic oscillator potential with natural frequencies $\omega_i (i = 1, 2, 3)$ characterize the degree of anisotropy and finite size

0305-4470/00/030487+20$30.00

effects. With respect to η_i, we can classify the dynamical behaviour of the system into the following four cases dependent on the degree of anisotropy:

Case 1 $\eta_1, \eta_2, \eta_3 > 1 \rightarrow \text{EIRD} = 0$

Case 2 $\eta_1, \eta_2 > 1 > \eta_3 \rightarrow \text{EIRD} = 1$

Case 3 $\eta_1 > 1 > \eta_2, \eta_3 \rightarrow \text{EIRD} = 2$

Case 4 $1 > \eta_1, \eta_2, \eta_3 \rightarrow \text{EIRD} = 3.$

As the temperature is lowered, dynamical dimensional reduction of the system characterized by the decrease of effective dimension can be observed. Particularly, in the presence of maximal anisotropy $1 \gg \eta_1 \gg \eta_2 \gg \eta_3$, EIRD decreases one by one from three to zero at the temperature $k_B T = \hbar\omega_1, \hbar\omega_2$ and $\hbar\omega_3$.

While the picture described above is of the generic nature of any quantum system, for particles that obey Bose statistics, the dimension of the dynamics of excited particles can also change in the form of condensation. BEC can also occur in separate steps in the presence of anisotropy reducing the effective dimension attributed to the excited modes of the system by one, two, or three at a time [10]. In this sense, the dimensional crossover associated with both the multistep condensation and the reduction of effective dimension due to frozen degrees of freedom can manifest themselves in a similar way in a finite system in spite of their different origin. This is the main subject discussed in this paper.

For the system with a finite size and number of atoms, the reduced chemical potential $\phi \equiv \beta(E_0 - \mu)$ does not strictly vanish at the critical temperature. Only in the thermodynamic limit, ϕ vanishes at the critical temperature and the specific heat develops the discontinuity in the derivative at the critical point [20]. In an isotropic system, the thermodynamic limit can be uniquely defined as discussed in many textbooks [4]. However, if we allow anisotropy in the system, there are three different ways of taking a thermodynamic limit. The three-dimensional limit: $\omega_1, \omega_2, \omega_3 \rightarrow 0$, while keeping $N\omega_1\omega_2\omega_3$ fixed. In this case, the system shows the critical behaviour of three dimensions and the corresponding three-dimensional critical temperature T_{3D} can be defined. The two-dimensional limit: $\omega_2\omega_3 \rightarrow 0$, while keeping $N\omega_2\omega_3$ fixed. The system shows the critical behaviour of two dimensions and the corresponding two-dimensional critical temperature T_{2D} can be defined. The one-dimensional limit: if we simply take $\omega_3 \rightarrow 0$, while keeping $N\omega_3$ fixed, the critical temperature vanishes. However, if we tune ω_3 a little slower such that $\omega_3 \sim \log(2N)/N \rightarrow 0$, the one-dimensional critical temperature T_{1D} can still be defined in this modified sense. We will discuss this issue again in section 3.1.

In the presence of strong anisotropy, the whole particle spectrum naturally splits into zero-, one-, two-, and three-dimensional excitations. The ground state is viewed as a zero-dimensional excitation. Let us denote the number of modes excited in the corresponding directions as N_0, N_1, N_2 and N_3, respectively. An n-dimensional condensation temperature T_{nD} $(n = 1, 2, 3)$ can be defined as the temperature at which all the n-dimensionally excited modes are saturated:

$$\text{three-dimensional} \quad N = N_3(T_{3D}) \tag{1}$$

$$\text{two-dimensional} \quad N = N_3(T_{2D}) + N_2(T_{2D}) \tag{2}$$

$$\text{one-dimensional} \quad N = N_3(T_{1D}) + N_2(T_{1D}) + N_1(T_{1D}). \tag{3}$$

One can see that the condensation temperatures defined above are equivalent to the critical temperatures if the appropriate n-dimensional thermodynamic limit is taken. This splitting of the excitation spectrum gives the basis of the rest of our analysis. Similar splitting was proposed in [10] for liquid helium. In a liquid, however, an occupation number of particles excited in a

particular direction is extremely difficult to observe. Furthermore, the validity of this splitting is by no means obvious for a strongly interacting system such as liquid helium. On the other hand, such a quantity is directly observable in atom trap experiments and, therefore, it deserves careful study. Moreover, as shown in section 3, occupation numbers N_1, N_2 and N_3 behave as if they were independent quantities and show similar behaviour when multistep crossover occurs. This result indicates the independent nature of each N_i for strongly anisotropic systems.

For a realistic system where $N, \omega_1, \omega_2, \omega_3$, are all finite and fixed, the physically observable temperature of interest is the crossover temperature at which the deviation from the bulk critical behaviour sets in. The crossover temperature is achieved when the correlation length reaches the size of the system since further ordering in this direction will be suppressed at this point. In the strongly anisotropic system in which $\omega_1, \omega_2 \gg \omega_3$ holds, $T_{1D}, T_{2D} \ll T_{3D}$ gives the necessary (but not sufficient) condition for the multistep condensation: the condensation into two, one-dimensional modes and into the ground state can occur in separate steps. The multistep condensation was discussed for a nonrelativistic ideal gas in a cavity [10], in a harmonic trap [24], and a relativistic ideal gas in a cavity [25].

In section 2, we study the excitation spectrum of anisotropic harmonic oscillators. We focus our attention to three different cases in which the equipotential surface has a prolate, oblate, and maximally anisotropic ellipsoidal shape. In section 3, we show that each case shows qualitatively different condensation behaviour. After introducing the condensation temperatures defined in the bulk limit, we focus on the multistep crossover behaviour of excited modes between different effective dimensions through BEC or dynamical reduction of EIRD. In particular, in a maximally anisotropic potential, the dimensional reduction can occur in three steps. In such a case, we show that each dimensional component behaves in a similar manner as a function of the reduced temperature defined near the corresponding crossover temperature. The possible effect of interactions is also discussed.

This paper deals with a nonrelativistic ideal Bose gas in anisotropic magnetic traps, and a companion paper deals with a relativistic ideal Bose gas in rectangular cavities [25]. Our calculations are focused on the occupation number and condensation temperature for each dimension. The effect of an interaction in the condensation process has been discussed many times in the literature. In principle, it can affect the dynamics of condensation considerably. For a weakly interacting gas, however, the averaged quantities such as condensation fractions and critical temperatures are relatively insensitive to the presence of interactions and the corrections to bulk ideal-gas values are well explained by the finite number correction [26,27]. On the other hand, interaction effects are known to affect higher moments such as specific heat significantly, and are considered to be essential to explain the observed specific heat data. Throughout the rest of the paper, we use units such that $k_B = \hbar = 1$ for brevity. The results in ordinary units can be easily reproduced by replacing $\omega \to \hbar\omega$ and $T \to k_B T$.

2. Anisotropic harmonic oscillator and excitation spectrum

For an anisotropic harmonic oscillator with oscillator frequencies $\omega_i (i = 1, 2, 3)$, the Hamiltonian has the form

$$H = \tfrac{1}{2} \sum_{i=1}^{3} (p_i^2 + \omega_i^2 x_i^2). \tag{4}$$

In this paper, we study cases where the frequencies ω_i are rationally related†. Whence there exist integers $k_i (i = 1, 2, 3)$ such that $\omega_i k_i = \omega (i = 1, 2, 3)$, where $\omega = \Omega (k_1 k_2 k_3)^{1/3}$ and

† This assumption of rationality is rather for the technical convenience and will not affect the physical results of this paper. Other methods can be found, for example, in [14, 24, 28].

$\omega_1\omega_2\omega_3 = \Omega^3$.

The energy level of an anisotropic harmonic oscillator is given by

$$E_n = \sum_{i=1}^{3} \omega_i (n_i + \tfrac{1}{2}). \tag{5}$$

We can also define the energy level modulo k_i as $n_i = k_i \nu_i + \lambda_i$, where $\nu_i \equiv [n_i/k_i]$, and [ ] denotes the integer part of the number inside the bracket. Then equation (5) can be written as

$$E_n = \omega M + \sum_{i=1}^{3} \omega_i \lambda_i + E_0 \tag{6}$$

where $M = \nu_1 + \nu_2 + \nu_3$. The first term in equation (6) corresponds to the isotropic harmonic oscillator Hamiltonian (see also appendix A). The ground state energy E_0 has the familiar form

$$E_0 = \frac{\omega_1 + \omega_2 + \omega_3}{2}. \tag{7}$$

2.1. Excitation spectrum

2.1.1. Prolate shape potential. First we discuss the case of anisotropy corresponding to $\omega_1 = \omega_2 > \omega_3$ (we simply choose here $k_1 = k_2 = 1 < k_3$). In such a case, the equipotential surface has a prolate shape. For a strong anisotropy $k_3 \gg 1$, two-step condensation can occur. In such a case, $\omega = \omega_1 = \omega_2$ and the energy eigenvalue is

$$E_n = \omega M + \omega_3 \lambda_3 + E_0. \tag{8}$$

For sufficiently large values of k_3, the whole energy spectrum can be split into the energy level of the ground state ($\bar{E}_n = 0$), one-dimensionally excited states ($\bar{E}_n = n_3\omega_3$; $n_3 = 1, 2, \ldots$), two-dimensionally excited states ($\bar{E}_n = n_1\omega_1 + n_3\omega_3$; $n_1 = 1, 2, \ldots, n_3 = 0, 1, \ldots$ and $n_2\omega_2 + n_3\omega_3$, $n_2 = 1, 2, \ldots, n_3 = 0, 1, \ldots$), and three-dimensionally excited states ($\bar{E}_n = n_1\omega_1 + n_2\omega_2 + n_3\omega_3$; $n_1, n_2 = 1, 2, \ldots, n_3 = 0, 1, \ldots$), where $\bar{E}_n \equiv E_n - E_0 = \omega M + \omega_3\lambda_3$ is the energy measured from the ground state. The number of particles excited in these dimensions are given, respectively, by

$$N_0 = \frac{z}{1 - z} \tag{9}$$

$$N_1 = \sum_{n_3=1}^{\infty} \frac{z}{\mathrm{e}^{n_3\eta_3} - z} \tag{10}$$

$$N_2 = \sum_{n_1=1, n_3=0}^{\infty} \frac{2z}{\mathrm{e}^{n_1\eta_1 + n_3\eta_3} - z} = \sum_{\lambda_3=0}^{k_3-1} \sum_{M=1}^{\infty} \frac{2Mz}{\mathrm{e}^{M\eta_1 + \lambda_3\eta_3} - z} \tag{11}$$

$$N_3 = \sum_{n_1=n_2=1, n_3=0}^{\infty} \frac{z}{\mathrm{e}^{n_1\eta_1 + n_2\eta_2 + n_3\eta_3} - z} = \sum_{\lambda_3=0}^{k_3-1} \sum_{M=2}^{\infty} \frac{(M-1)M}{2} \frac{z}{\mathrm{e}^{M\eta_1 + \lambda_3\eta_3} - z} \tag{12}$$

where $z \equiv \mathrm{e}^{\beta(\mu - E_0)}$ is the (reduced) fugacity. The factor 2 in equation (11) accounts for the symmetry between the first and second axes. These expressions can be further simplified in the following manner.

For one dimension,

$$N_1 = \sum_{n_3=1}^{\infty} \frac{z\mathrm{e}^{-n_3\eta_3}}{1 - z\mathrm{e}^{-n_3\eta_3}} = \sum_{l=1}^{\infty} \frac{z^l \mathrm{e}^{-l\eta_3}}{1 - \mathrm{e}^{-l\eta_3}} \tag{13}$$

$$= \frac{g_1(z\mathrm{e}^{-\eta_3/2})}{\eta_3} + \cdots \tag{14}$$

where $g_p(z) = \sum_{n=1}^{\infty} \frac{z^n}{n^p}$ is the Bose–Einstein function. We used equation (B4) to obtain the second line from the first line.

For two-dimensional excitations, making use of equation (B2), equation (11) can be written as

$$\begin{aligned} N_2 &= 2\sum_{\lambda_3=0}^{k_3-1}\sum_{M=1}^{\infty}\sum_{l=1}^{\infty} M z^l \mathrm{e}^{-l(M\eta_1+\lambda_3\eta_3)} \\ &= 2\sum_{l=1}^{\infty} \frac{z^l \mathrm{e}^{-l\eta_1}}{(1-\mathrm{e}^{-l\eta_1})(1-\mathrm{e}^{-l\eta_3})} \\ &= 2\sum_{l=1}^{\infty} \frac{z^l \mathrm{e}^{-l(\eta_1-\eta_3)/2}}{l^2\eta_1\eta_3} - \left(k_3+\frac{1}{k_3}\right)\sum_{l=1}^{\infty}\frac{z^l \mathrm{e}^{-l(\eta_1-\eta_3)/2}}{12} + \cdots \\ &= \frac{2g_2(z\mathrm{e}^{-(\eta_1-\eta_3)/2})}{\eta_1\eta_3} - \frac{k_3 g_0(z\mathrm{e}^{-(\eta_1-\eta_3)/2})}{12} + \cdots . \end{aligned} \tag{15}$$

To obtain the third line from the second line, we used equation (B5).

For three-dimensional excitations, equation (12) gives

$$\begin{aligned} N_3 &= \sum_{\lambda_3=0}^{k_3-1}\sum_{M=2}^{\infty}\sum_{l=1}^{\infty} \frac{(M-1)M}{2} z^l \mathrm{e}^{-l(M\eta_1+\lambda_3\eta_3)} \\ &= \sum_{l=1}^{\infty} z^l \frac{\mathrm{e}^{-2l\eta_1}}{(1-\mathrm{e}^{-l\eta_1})^2(1-\mathrm{e}^{-l\eta_3})} \\ &= \sum_{l=1}^{\infty} \frac{z^l \mathrm{e}^{-l(\eta_1-\eta_3/2)}}{l^3\eta_1^2\eta_3} - \sum_{l=1}^{\infty}\frac{z^l \mathrm{e}^{-l(\eta_1-\eta_3/2)}}{12l\eta_3} + \cdots \\ &= \frac{g_3(z\mathrm{e}^{-(\eta_1-\eta_3/2)})}{\eta_1^2\eta_3} - \frac{g_1(z\mathrm{e}^{-(\eta_1-\eta_3/2)})}{12\eta_3} + \cdots . \end{aligned} \tag{16}$$

2.1.2. Oblate shape potential. Next we discuss the case of anisotropy corresponding to an oblate shape potential $\omega_1 > \omega_2 = \omega_3$ ($k_1 = 1 < k_2 = k_3$). In this case, $\omega = \omega_1$ and

$$\bar{E}_n = \omega M + \omega_2(\lambda_2 + \lambda_3). \tag{17}$$

The number of particles excited in these dimensions are given, respectively, by

$$N_0 = \frac{z}{1-z} \tag{18}$$

$$N_1 = \sum_{n_2=1}^{\infty} \frac{2z}{\mathrm{e}^{n_2\eta_2} - z} \tag{19}$$

$$N_2 = \sum_{n_2=1,n_3=1}^{\infty} \frac{z}{\mathrm{e}^{n_2\eta_2+n_3\eta_3} - z} = \sum_{M=2}^{\infty} \frac{(M-1)z}{\mathrm{e}^{M\eta_2} - z} \tag{20}$$

$$N_3 = \sum_{n_1=1,n_2=0,n_3=0}^{\infty} \frac{z}{\mathrm{e}^{n_1\eta_1+n_2\eta_2+n_3\eta_3} - z} = \sum_{n_1=1}^{\infty}\sum_{M=0}^{\infty} \frac{(M+1)z}{\mathrm{e}^{n_1\eta_1+M\eta_2} - z} \tag{21}$$

where the factor 2 in equation (19) is due to the symmetry between the second and third axes.

Compared with equation (14), we obtain

$$N_1 = \frac{2g_1(z\mathrm{e}^{-\eta_2/2})}{\eta_2} + \cdots \tag{22}$$

in the present case.

The number of particles excited two-dimensionally on the x_2–x_3 plane can be written as

$$N_2 = \sum_{l=1}^{\infty}\sum_{M=2}^{\infty}(M-1)z^l \mathrm{e}^{-lM\eta_2} = \sum_{l=1}^{\infty}\frac{z^l \mathrm{e}^{-2l\eta_2}}{(1-\mathrm{e}^{-l\eta_2})^2} = \frac{g_2(z\mathrm{e}^{-\eta_2})}{\eta_2^2} + \cdots. \tag{23}$$

For three-dimensional excitations, equation (21) gives

$$\begin{aligned} N_3 &= \sum_{l=1}^{\infty} z^l \frac{\mathrm{e}^{-l\eta_1}}{(1-\mathrm{e}^{-l\eta_1})(1-\mathrm{e}^{-l\eta_2})^2} \\ &= \frac{g_3(z\mathrm{e}^{-(\eta_1/2-\eta_2)})}{\eta_1\eta_2^2} - \frac{g_1(z\mathrm{e}^{-(\eta_1/2-\eta_2)})}{24}\left(\frac{\eta_1^2+2\eta_2^2}{\eta_1\eta_2^2}\right) + \cdots. \end{aligned} \tag{24}$$

2.1.3. Maximally anisotropic potential. For anisotropies $\omega_1 > \omega_2 > \omega_3$ with $k_1 = 1 \ll k_2 \ll k_3$, $\omega = \omega_1$ and

$$\bar{E}_n = \omega M + \omega_2\lambda_2 + \omega_3\lambda_3. \tag{25}$$

The number of excited modes in the corresponding dimensions can be defined by

$$N_1 = \sum_{n_3=1}^{\infty}\frac{z}{\mathrm{e}^{n_3\eta_3}-z} \tag{26}$$

$$N_2 = \sum_{n_2=1,n_3=0}^{\infty}\frac{z}{\mathrm{e}^{n_2\eta_2+n_3\eta_3}-z} \tag{27}$$

$$N_3 = \sum_{n_1=1,n_2=n_3=0}^{\infty}\frac{z}{\mathrm{e}^{n_1\eta_1+n_2\eta_2+n_3\eta_3}-z} = \sum_{\lambda_2=0}^{k_2-1}\sum_{\lambda_3=0}^{k_3-1}\sum_{M=1}^{\infty}\frac{M(M+1)}{2}\frac{z}{\mathrm{e}^{M\eta_1+\lambda_2\eta_2+\lambda_3\eta_3}-z}. \tag{28}$$

For the two-dimensional case, following equation (15),

$$\begin{aligned} N_2 &= \sum_{\lambda_3=0}^{\kappa-1}\sum_{M=1}^{\infty}\sum_{l=1}^{\infty} M z^l \mathrm{e}^{-l(M\eta_2+\lambda_3\eta_3)} \\ &= \sum_{l=1}^{\infty}\frac{z^l\mathrm{e}^{-l\eta_2}}{(1-\mathrm{e}^{-l\eta_2})(1-\mathrm{e}^{-l\eta_3})} \\ &= \sum_{l=1}^{\infty}\frac{z^l\mathrm{e}^{-\eta_2/2}}{l^2\eta_2\eta_3} - \left(\kappa+\frac{1}{\kappa}\right)\sum_{l=1}^{\infty}\frac{z^l\mathrm{e}^{-\eta_2/2}}{24} + \cdots \\ &= \frac{g_2(z\mathrm{e}^{-\eta_2/2})}{\eta_2\eta_3} - \frac{\kappa g_0(z\mathrm{e}^{-\eta_2/2})}{24} + \cdots \end{aligned} \tag{29}$$

where $\kappa \equiv k_3/k_2$.

For three-dimensional excitations, equation (28) gives

$$\begin{aligned} N_3 &= \sum_{l=1}^{\infty} z^l \frac{\mathrm{e}^{-l\eta_1}}{(1-\mathrm{e}^{-l\eta_1})(1-\mathrm{e}^{-l\eta_2})(1-\mathrm{e}^{-l\eta_3})} \\ &= \sum_{l=1}^{\infty}\frac{z^l\mathrm{e}^{-l(\eta_1-\eta_2-\eta_3)/2}}{l^3\eta_1\eta_2\eta_3} - \sum_{l=1}^{\infty}\frac{z^l\mathrm{e}^{-l(\eta_1-\eta_2-\eta_3)/2}}{24l}\left(\frac{\eta_1^2+\eta_2^2+\eta_3^2}{\eta_1\eta_2\eta_3}\right) + \cdots \\ &= \frac{g_3(z\mathrm{e}^{-(\eta_1-\eta_2-\eta_3)/2})}{\eta_1\eta_2\eta_3} - \frac{g_1(z\mathrm{e}^{-(\eta_1-\eta_2-\eta_3)/2})}{24}\left(\frac{\eta_1^2+\eta_2^2+\eta_3^2}{\eta_1\eta_2\eta_3}\right) + \cdots. \end{aligned} \tag{30}$$

3. Finite size effects and dimensional crossover behaviour

3.1. Bulk behaviour

The bulk three-dimensional condensation temperature is defined in the thermodynamic limit $\eta_i \to 0$ $(i = 1, 2, 3)$ and $N \to \infty$, while η_1/η_3 and η_2/η_3 remain fixed. The dominant term is given by the first term in N_3 and the critical temperature satisfies

$$N = \frac{T_{3D}^3}{\omega_1\omega_2\omega_3}\zeta(3). \tag{31}$$

Therefore

$$T_{3D} = \left(\frac{N\omega_1\omega_2\omega_3}{\zeta(3)}\right)^{1/3}. \tag{32}$$

The two-dimensional limit is given by $\eta_2, \eta_3 \to 0$, $N \to \infty$, but $\eta_1 \gg 1$. In such a case, the dominant term in particle number is N_2 and the critical temperature T_{2D} is defined by

$$N = \frac{T_{2D}^2}{\omega_2\omega_3} g_2(\mathrm{e}^{-(\omega_2+\omega_3)/2T_{2D}}) = \frac{T_{2D}^2}{\omega_2\omega_3}\zeta(2) + \cdots. \tag{33}$$

Thus we have

$$T_{2D} = \left(\frac{N\omega_2\omega_3}{\zeta(2)}\right)^{1/2}. \tag{34}$$

For one-dimensional limit $\eta_3 \to 0$, $N \to \infty$, but $\eta_1, \eta_2 \gg 1$, the dominant term in particle number is N_1. The condensation temperature is defined by

$$N = \frac{T_{1D}}{\omega_3} g_1(\mathrm{e}^{-\omega_3/2T_{1D}}). \tag{35}$$

To leading order in η_3^{-1}, equation (14) can be approximated as $N_1 \sim \frac{T}{\omega_3}\log\frac{2T}{\omega_3}$. Thus the one-dimensional condensation temperature T_{1D} is defined by

$$N = \frac{T_{1D}}{\omega_3}\log\frac{2T_{1D}}{\omega_3} \tag{36}$$

which gives

$$T_{1D} = \frac{N\omega_3}{\log(2N)} \tag{37}$$

for large N. Note that in the thermodynamic limit $N \to \infty$, while $N\omega_3$ remains fixed, T_{1D} vanishes.

In figure 1, we plot T_{1D}, T_{2D} and T_{3D} as a function of the anisotropy parameter k_3. In an isotropic and weakly isotropic case ($k_3 \sim 1$), $T_{3D} < T_{1D}, T_{2D}$, and the condensation is directly into the ground state. As anisotropy is increased ($k_3 \gg 10^3$), $T_{1D}, T_{2D} < T_{3D}$ is achieved. This is the regime where various multistep behaviours can take place.

In terms of the bulk condensation temperatures we obtained in section 3.1 as $T_{1D} = N\omega_3/\log(2N)$, $T_{2D} = (N\omega_2\omega_3/2\zeta(2))^{1/2}$, and $T_{3D} = (N\omega_1\omega_2\omega_3/\zeta(3))^{1/3}$, the conditions (A) $T_{1D} \ll T_{2D}$, (B) $T_{2D} \ll T_{3D}$, and (C) $T_{1D} \ll T_{3D}$ give constraints for k_3 and κ as follows:

$$\begin{aligned} &\text{(A)} \quad \kappa \gg \frac{N\zeta(2)}{(\log(2N))^2} \\ &\text{(B)} \quad k_3^2/\kappa \gg \frac{N\zeta(3)^2}{\zeta(2)^3} \\ &\text{(C)} \quad k_3\kappa \gg \frac{N^2}{(\log(2N))^3}. \end{aligned} \tag{38}$$

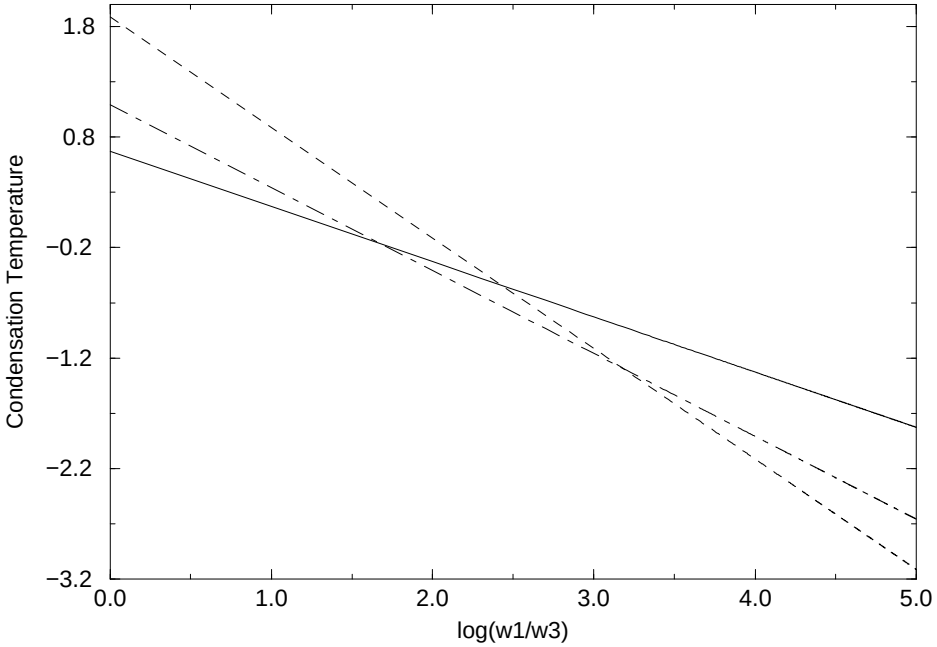

Figure 1. The condensation temperatures T_{1D} (solid line), T_{2D} (dashed line), and T_{3D} (dot-dashed line) are shown as a function of k_3. $N = 10^4$, $\omega_1 = 0.5$ and k_2 is also varied as $k_2^{\,2} = k_3$. The logarithmic scale is used for both axes.

Since (B) $T_{2D} \ll T_{3D}$ implies $T_{3D} \ll \omega_1$, three-step BEC never occurs in harmonic traps. In figure 2, different condensation behaviours corresponding to various anisotropy parameters ω_1/ω_2 and ω_2/ω_3 are shown. The vertical axis corresponds to the prolate-shape potential studied in section 3.2.1 (this case was studied in [24]). In such a potential, two-step BEC can be seen. The horizontal axis corresponds to the oblate-shape potential discussed in section 3.2.2, where we show that there is no multistep condensation in this case. The more general class of anisotropic case will be discussed in section 3.2.3. The combined effect of dynamical dimensional reduction and two-step BEC in such a potential can appear in three steps.

3.2. Dimensional crossover and condensation

For a highly anisotropic trap, the three-dimensional crossover temperature T_{3D}^* should be reached when the correlation length is in the order of the size of the ground state wavefunction in the most confining direction. Spreading of the wavefunction can be characterized by $L_i \equiv \sqrt{h/m\omega_i}$ (for $i = 1, 2, 3$) [29, 30]. Hence the above condition is equivalent to $\xi(T_{3D}^*) \sim \lambda_{\theta dB}/\sqrt{t_3} \sim L_1$, where $\lambda_{\theta dB} \equiv h/\sqrt{2\pi mkT}$ is the thermal de Broglie wavelength, and $t_3 \equiv |T_{3D}^* - T_{3D}|/T_{3D}$. This will give us the crude estimate of T_{3D}^* as

$$|T_{3D}^* - T_{3D}| \sim \left(\frac{k_3\zeta(3)}{N}\right)^{1/3} T_{3D}. \tag{39}$$

3.2.1. Two-step condensation. For a prolate-shape potential discussed in section 2.1.1, we expand the whole particle spectrum with respect to η_1 and η_3 and obtain

$N = N_0 + N_1 + N_2 + N_3$

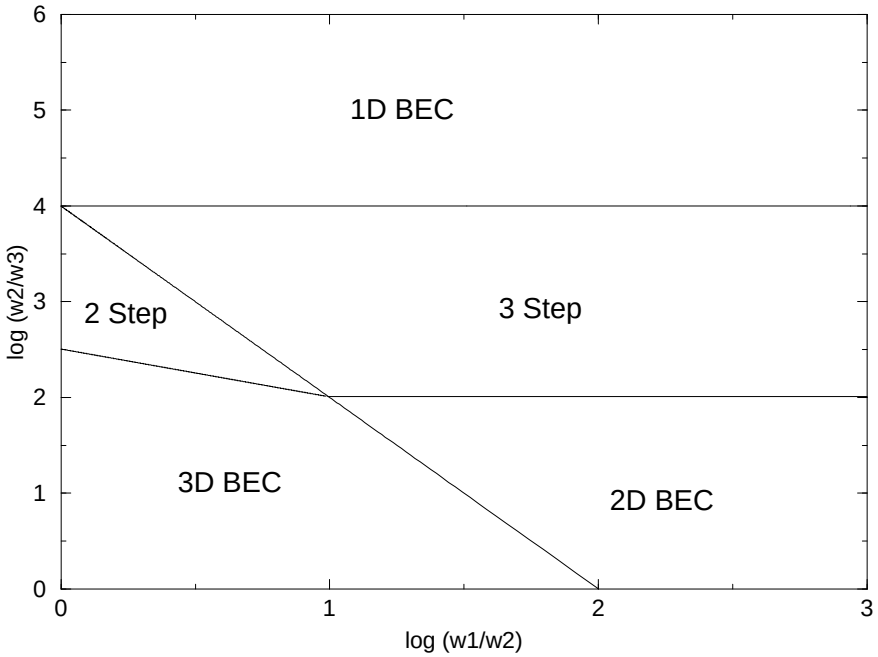

Figure 2. Different condensation behaviours corresponding to different anisotropy parameters ω_1/ω_2 and ω_2/ω_3 are indicated. $N = 10^4$ is chosen. The logarithmic scale is used for both horizontal and vertical axes. $\zeta(2)$ and $\zeta(3)$ are approximated as one for simplicity.

$$
\begin{aligned}
&= g_0(z) + \frac{g_1(z\mathrm{e}^{-\eta_3/2})}{\eta_3} + \frac{2g_2(z\mathrm{e}^{-\eta_1/2})}{\eta_1\eta_3} + \frac{g_3(z\mathrm{e}^{-\eta_1})}{\eta_1^2\eta_3} + \cdots \\
&= g_0(z) + \frac{g_1(z)}{\eta_3} + \frac{2g_2(z)}{\eta_1\eta_3} + \frac{g_3(z)}{\eta_1^2\eta_3} \\
&\quad - \frac{g_0(z)}{\eta_3}\frac{\eta_3}{2} - \frac{2g_1(z)}{\eta_1\eta_3}\frac{\eta_1}{2} - \frac{g_2(z)}{\eta_1^2\eta_3}\eta_1 \\
&\quad + \frac{g_0(z)}{\eta_1\eta_3}\left(\frac{\eta_1}{2}\right)^2 + \frac{g_1(z)}{\eta_1^2\eta_3}\frac{\eta_1^2}{2} - \frac{g_0(z)}{\eta_1^2\eta_3}\frac{\eta_1^3}{6} + \cdots .
\end{aligned} \tag{40}
$$

This expression can be simplified to give

$$
N\eta_3 = \frac{g_3(z)}{\eta_1^2} + \frac{g_2(z)}{\eta_1} + \frac{g_1(z)}{2} + \cdots . \tag{41}
$$

Writing $z = \mathrm{e}^{-\phi}$ and expanding equation (41) with respect to ϕ gives

$$
N\eta_3 = \frac{\zeta(3)}{\eta_1^2} + \frac{\zeta(2)}{\eta_1} - \frac{\zeta(2)\phi}{\eta_1^2} + \cdots \tag{42}
$$

where we used an asymptotic expansion of the Bose–Einstein function $g_3(\mathrm{e}^{-\alpha}) \sim \zeta(3) - \zeta(2)\alpha + \frac{1}{2}(\frac{3}{2} - \log\alpha)\alpha^2 + \cdots$ and $g_2(\mathrm{e}^{-\alpha}) \sim \zeta(2) + (\log\alpha - 1)\alpha + \cdots$ for small α [4].

The correlation length ξ of an ideal Bose gas is given by $\xi = \lambda_{\theta dB}/2\sqrt{\pi\phi}$ [31]. In terms of scaling parameters $x_i(T) \equiv \phi(T)/\eta_i (i = 1, 2, 3)$, the above argument implies that T_{3D}^* is achieved when $x_1(T_{3D}^*) \equiv c_1$, where c_1 is some constant in the order of unity. Inserting this

into equation (42) gives

$$N = \frac{\zeta(3)}{\eta_1^2\eta_3} + \frac{\zeta(2)(1-c_1)}{\eta_1\eta_3} + \cdots \qquad \text{at} \quad T = T_{3D}^*. \tag{43}$$

Thus we have

$$\frac{T_{3D}^*}{T_{3D}} = 1 + \frac{c_1 - 1}{3}\frac{\zeta(2)}{\zeta(3)^{2/3}}\left(\frac{k_3}{N}\right)^{1/3}. \tag{44}$$

This result gives the same correction term proportional to $(k_3/N)^{1/3}$ as in equation (39) obtained by heuristic arguments.

The one-dimensional condensation temperature T_{1D} is defined in equation (35) in the limit of small η_3 and the vanishing reduced chemical potential ϕ; finite size effects on T_{1D} originate in finiteness of both η_3 and ϕ. At one-dimensional crossover temperature T_{1D}^*, correlation length reaches the size of the ground state wavefunction in the least confining direction, namely, along the third axis in the present case. Thus $\xi(T_{1D}^*) \sim L_3$, or equivalently, $x_3(T_{1D}^*) \equiv c_3 = \mathrm{O}(1)$. Then from the second line in equation (40), we obtain

$$N = \frac{g_1(\mathrm{e}^{-(1+2c_3)\eta_3/2})}{\eta_3} + \frac{2g_2(\mathrm{e}^{-(k_3+2c_3)\eta_3/2})}{\eta_1\eta_3} + \frac{g_3(\mathrm{e}^{-(k_3+c_3)\eta_3})}{\eta_1^2\eta_3} + \cdots. \tag{45}$$

In the limit $\eta_3 \to 0$, only the first term dominates and we obtain the crossover temperature as

$$N = -\frac{T_{1D}^*}{\omega_3}\log(1 - \mathrm{e}^{-(1+2c_3)\omega_3/2T_{1D}^*}) = \frac{T_{1D}^*}{\omega_3}\log\frac{2T_{1D}^*}{(1+2c_3)\omega_3}. \tag{46}$$

For large N, this gives

$$T_{1D}^* = \frac{N\omega_3}{\log[2N/(1+2c_3)]}. \tag{47}$$

Note that $T_{1D}^* > T_{1D}$ holds.

The conditions (C) in equation (38) and $\omega_1 < T_{1D}$ are satisfied if

$$\frac{N}{(\log(2N))^{3/2}} < k_3 < \frac{N}{(\log(2N))}. \tag{48}$$

In such a case, two-step condensation leading to the condensation into the ground state can be seen whereas the system is effectively still three-dimensional. In figures 3–6, the condensation fractions $N_i/N (i = 0, 1, 2, 3)$ as a function of temperature are plotted. At high temperature, three-dimensionally excited states dominate, as expected from the density of states which grows as M^2, where M is the number of degeneracy of an isotropic harmonic oscillator appeared in equation (6).

In the isotropic case (figure 3), condensation is only into the ground state. Due to the finite size effects, condensation already starts before the critical temperature is reached. In a strongly anisotropic case, as in figure 4, two-step condensation can be seen. T_{3D}^* determines the onset of condensation into one-dimensionally excited states. At T_{3D}^* the ground state fraction is negligibly small. Condensation into the ground state will not start until T_{1D}^* is reached.

In the multistep process peculiar to the highly anisotropic system, when the correlation length reaches the size of the system, the dynamics shows the crossover to the low-dimensional one before the actual phase transition occurs. In this sense, the critical temperature is never observed in such a process and the quantity directly relevant to the observation is the crossover temperature, the temperature at which the finite size correction sets in. For practical purposes, this is often replaced by including the finite size correction as the term proportional to the power of $1/N$ whereas the chemical potential is set to the ground state energy [32]. Strictly speaking, however, since the chemical potential never reaches the ground state energy in the

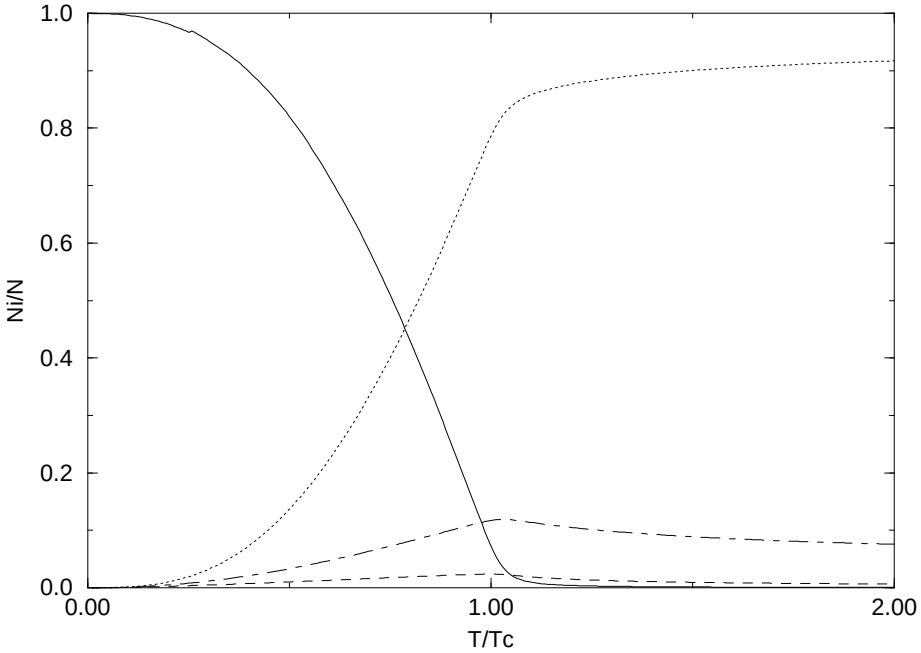

Figure 3. The condensation fractions N_0/N (solid curve), N_1/N (dashed curve), N_2/N (dot-dashed curve), N_3/N (dotted curve) as a function of the temperature for an isotropic trap are plotted. The same symbols are used in figures 4–7. $\omega_1 = 0.1$, $\omega_2 = 0.1$, $\omega_3 = 0.1$ and $N = 1000$ are chosen. $T_c = 0.94$ is the three-dimensional critical temperature in equation (32).

finite system, the meaning of this correction has some ambiguity. The difference between the crossover temperature and the finite size-corrected critical temperature in the present axially symmetric trap case is given by

$$\frac{\Delta T}{T_{3D}} = \frac{c_1}{3}\frac{\zeta(2)}{\zeta(3)^{2/3}}\left(\frac{k_3}{N}\right)^{1/3}. \tag{49}$$

While this is fairly small for an isotropic or weakly anisotropic case: $\Delta T/T_{3D} \sim 0.024$ for $k_3 = 1$, it is no longer so for a strongly anisotropic case: $\Delta T/T_{3D} \sim 0.24$ for $k_3 = 10^3$ as used in figure 4, where $c_1 = 1$, $N = 10^4$ for both cases. The ordinary finite size correction significantly underestimates the results in the latter case†. For these reasons, we focus our discussions on crossover temperatures in this paper. We should also note that there is a slight amount of ambiguity in the choice of c_i $(i = 1, 2, 3)$. In general, the correlation length ξ is a complicated function of the temperature away from the critical value and the reliable choice is obtained by the numerical fitting. We will simply put c_i $(i = 1, 2, 3) = 1$ for our comparison with numerical data for brevity.

3.2.2. Two-dimensional condensation. For an oblate shape potential discussed in section 2.1.2, assuming $\eta_1 \gg 1$ we obtain

$$\begin{aligned} N &= N_0 + N_1 + N_2 + N_3 \\ &= g_0(z) + \frac{2g_1(z\mathrm{e}^{-\eta_2/2})}{\eta_2} + \frac{g_2(z\mathrm{e}^{-\eta_2})}{\eta_2^2} + \cdots. \end{aligned} \tag{50}$$

† Since the boundary condition in the harmonic potential corresponds to the one in the Neumann boundary condition, the surface correction increases the density of states and hence decreases the critical temperature.

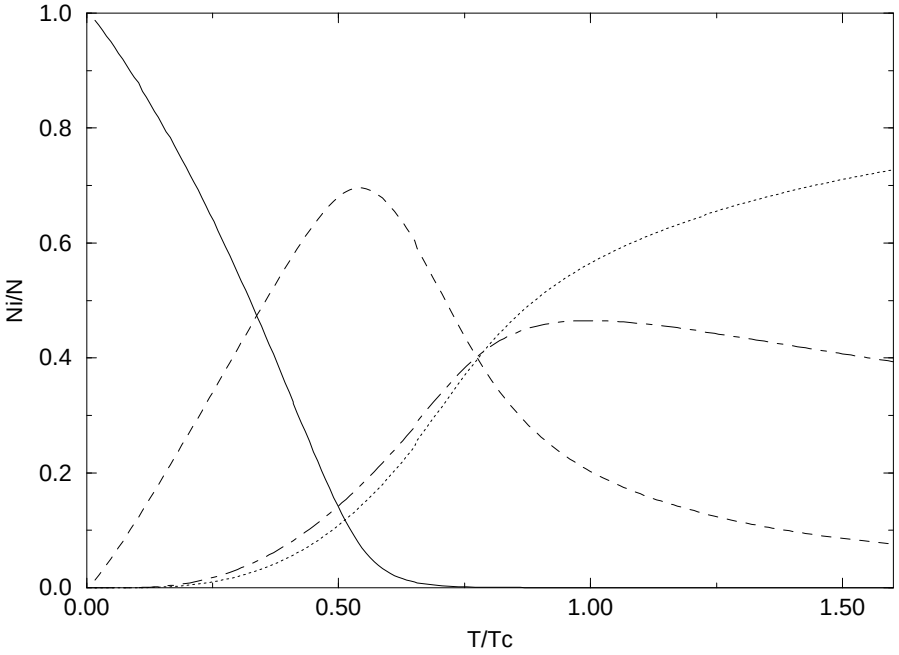

Figure 4. The condensation fractions for a prolate shape anisotropic trap are plotted. $\omega_1 = 0.3$, $\omega_2 = 0.3$, $\omega_3 = 0.0003$ and $N = 10^4$ are chosen. Two-step condensation occurs in this case. $T_c = T^*_{3D} = 0.61$ from equation (44) and $T^*_{1D} = 0.34$ from equation (47). c_1 and c_3 are set equal to one. Note that EIRD = 3 during the whole two-step BEC process.

The two-dimensional crossover temperature T^*_{2D} can be defined when the correlation length reaches the size of the ground state wavefunction along the second axis. Thus we have $\xi(T^*_{2D}) \sim L_2$ or equivalently, $x_2(T^*_{2D}) \equiv c_2 = \mathrm{O}(1)$. Then from equation (50) we obtain

$$N = \frac{g_2(\mathrm{e}^{-(1+c_2)\eta_2})}{\eta_2^2} + \frac{2g_1(\mathrm{e}^{-(1+2c_2)\eta_2/2})}{\eta_2} + \cdots \tag{51}$$

at $T = T^*_{2D}$. Expanding in terms of η_2, we obtain T^*_{2D} as

$$\begin{aligned} N &= \frac{\zeta(2)}{\eta_2^2} - \frac{1+c_2}{\eta_2} + \frac{(1+c_2)\log[\eta_2(1+c_2)]}{\eta_2} - \frac{2\log(\eta_2 c_2)}{\eta_2} \\ &= \frac{T^{*2}_{2D}\zeta(2)}{\omega_2^2} - \frac{T^*_{2D}}{\omega_2} \\ &\quad \times \left[(1+c_2) + (1+c_2)\log\left(\frac{T^*_{2D}}{\omega_2(1+c_2)}\right) + 2\log\left(\frac{T^*_{2D}}{\omega_2 c_2}\right)\right] + \cdots \end{aligned} \tag{52}$$

for $\eta_2, \eta_3 \ll 1$. For large N and $c_2 = 1$, this gives

$$\frac{T^*_{2D}}{T_{2D}} = 1 + \left(\frac{\kappa}{N\zeta(2)}\right)^{1/2} \log\left(\frac{N}{\kappa\zeta(2)}\right). \tag{53}$$

As explained in section 3.1, condensation into N_2 does not occur in harmonic traps. For an oblate shape potential, the system dynamics freezes out along the first axis at $T = \omega_1$. Therefore, the dynamics of the system at $T < \omega_1$ is two-dimensional. Ordinary two-dimensional BEC can still be observed as long as $T_{2D} < \omega_1$. This condition requires $k_3 > (N/\zeta(2))^{1/2}$. In figure 5, two-dimensional BEC in this parameter regime is shown.

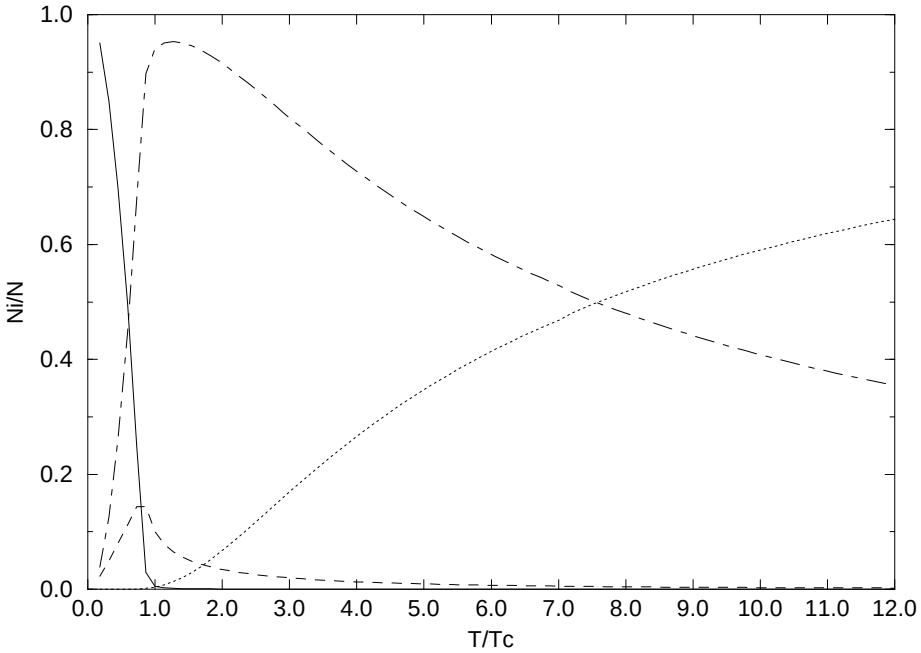

Figure 5. The condensation fractions for an oblate shape anisotropic trap are plotted. $\omega_1 = 0.3$, $\omega_2 = 0.002$, $\omega_3 = 0.002$ and $N = 10^3$ are chosen. $T_c = T^*_{2D} = 0.057$ is the two-dimensional crossover temperature in equation (53). c_2 is set equal to one. The system shows the dimensional reduction from three to two dimensions at $T = \omega_1 = 0.3$. Hence the accumulation of particles into N_2 from N_3 is not the result of condensation. At $T < \omega_1$, the system shows the ordinary two-dimensional condensation into the ground state.

3.2.3. Three-step dimensional reduction. For a general class of the anisotropic potential discussed in section 2.1.3, a three-step process can be observed. We expand each N_i with respect to η_1, η_2, η_3 and obtain

$$\begin{aligned} N &= N_0 + N_1 + N_2 + N_3 \\ &= g_0(z) + \frac{g_1(z\mathrm{e}^{-\eta_3/2})}{\eta_3} + \frac{g_2(z\mathrm{e}^{-\eta_2/2})}{\eta_2\eta_3} - \frac{\kappa}{24} g_0(z\mathrm{e}^{-\eta_2/2}) + \frac{g_3(z\mathrm{e}^{-(\eta_1-\eta_2-\eta_3)/2})}{\eta_1\eta_2\eta_3} \\ &\quad - \frac{g_1(z\mathrm{e}^{-(\eta_1-\eta_2-\eta_3)/2})}{24}\left(\frac{\eta_1^2+\eta_2^2+\eta_3^2}{\eta_1\eta_2\eta_3}\right) + \cdots \\ &= \frac{g_3(z)}{\eta_1\eta_2\eta_3} + \frac{g_2(z)}{\eta_2\eta_3} - \frac{g_2(z)}{\eta_1\eta_2\eta_3}\frac{\eta_1-\eta_2-\eta_3}{2} + \cdots . \end{aligned} \tag{54}$$

Expanding equation (54) with respect to $\phi = -\log z$, gives

$$N = \frac{\zeta(3)}{\eta_1\eta_2\eta_3} + \frac{\zeta(2)}{2}\left(\frac{1}{\eta_1\eta_2} + \frac{1}{\eta_2\eta_3} + \frac{1}{\eta_3\eta_1}\right) - \frac{\zeta(2)\phi}{\eta_1\eta_2\eta_3}\cdots . \tag{55}$$

As discussed in section 3.2.1, $x_1(T^*_{3D}) \equiv c_1 = \mathrm{O}(1)$ holds at $T = T^*_{3D}$. Inserting this into equation (55) gives

$$N = \frac{\zeta(3)}{\eta_1\eta_2\eta_3} + \frac{\zeta(2)}{2}\left[\frac{1}{\eta_1\eta_2} + \frac{1}{\eta_2\eta_3}\left(\frac{1}{2} - c_1\right) + \frac{1}{\eta_3\eta_1}\right] + \cdots \qquad \text{at} \quad T = T^*_{3D}. \tag{56}$$

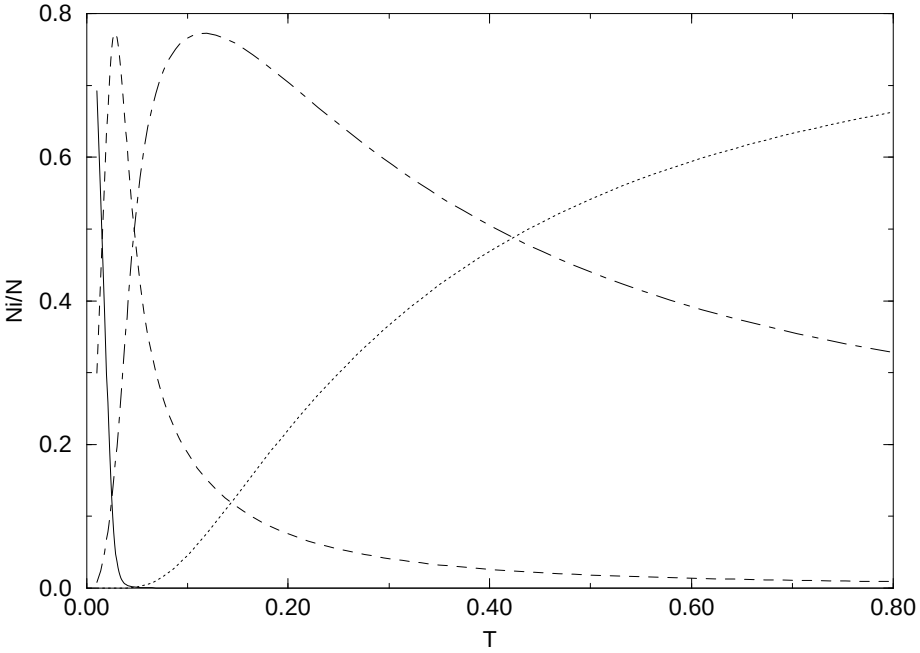

Figure 6. The condensation fractions for a maximally anisotropic trap are plotted. Three-step dimensional reduction can be seen. $\omega_1 = 0.3$, $\omega_2 = 0.02$, $\omega_3 = 0.0004$ and $N = 5 \times 10^3$ are used. $T^*_{3D} = 0.17$, $T^*_{2D} = 0.06$ and $T^*_{1D} = 0.02$ are crossover temperatures defined in equations (57), (60) and (47), respectively. $c_1 = c_2 = c_3 = 1$ are used. The system shows the dimensional reduction at $T = \omega_1 = 0.3$ similar to figure 5, and behaves two-dimensionally near $T < 0.3$. Therefore, the accumulation of particles into N_2 from N_3 is not the result of condensation. For $T < \omega_1$, the system shows two-step BEC at T^*_{2D} into one-dimensionally excited states and at T^*_{1D} into the ground state.

Thus we have

$$\frac{T^*_{3D}}{T_{3D}} = 1 + \frac{c_1 - 1/2}{3}\frac{\zeta(2)}{\zeta(3)^{2/3}}\left(\frac{k_2 k_3}{N}\right)^{1/3}. \tag{57}$$

The crossover temperature T^*_{2D} associated with two-dimensional BEC can be defined if $T^*_{2D} < \omega_1$†. Then from equation (54) we obtain

$$N = \frac{g_2(\mathrm{e}^{-\eta_2(1/2+c_2)})}{\eta_2\eta_3} + \frac{g_1(\mathrm{e}^{-\eta_2(1/2+c_2)})}{\eta_3} + \frac{\mathrm{e}^{-\eta_1/2}}{\eta_1\eta_2\eta_3} + \frac{\log(1-\mathrm{e}^{-\eta_1/2})\eta_1}{24\eta_2\eta_3} + \cdots \tag{58}$$

at $T = T^*_{2D}$. When η_1 becomes large, only the first two terms dominate and we obtain the crossover temperature as

$$\begin{aligned} N &= \frac{\zeta(2)}{\eta_2\eta_3} - \frac{1/2+c_2}{\eta_3} + \frac{(1/2+c_2)\log[\eta_2(1/2+c_2)]}{\eta_3} - \frac{\log(\eta_2 c_2)}{\eta_3} + \cdots \\ &= \frac{T^{*2}_{2D}\zeta(2)}{\omega_2\omega_3} - \frac{T^*_{2D}}{\omega_3} \\ &\quad \times\left[(1/2+c_2) + (1/2+c_2)\log\left(\frac{T^*_{2D}}{\omega_2(1/2+c_2)}\right) + \log\left(\frac{T^*_{2D}}{\omega_2 c_2}\right)\right] + \cdots \end{aligned} \tag{59}$$

† Thus the system behaves effectively two-dimensional (EIRD = 2) at $T = T^*_{2D}$.

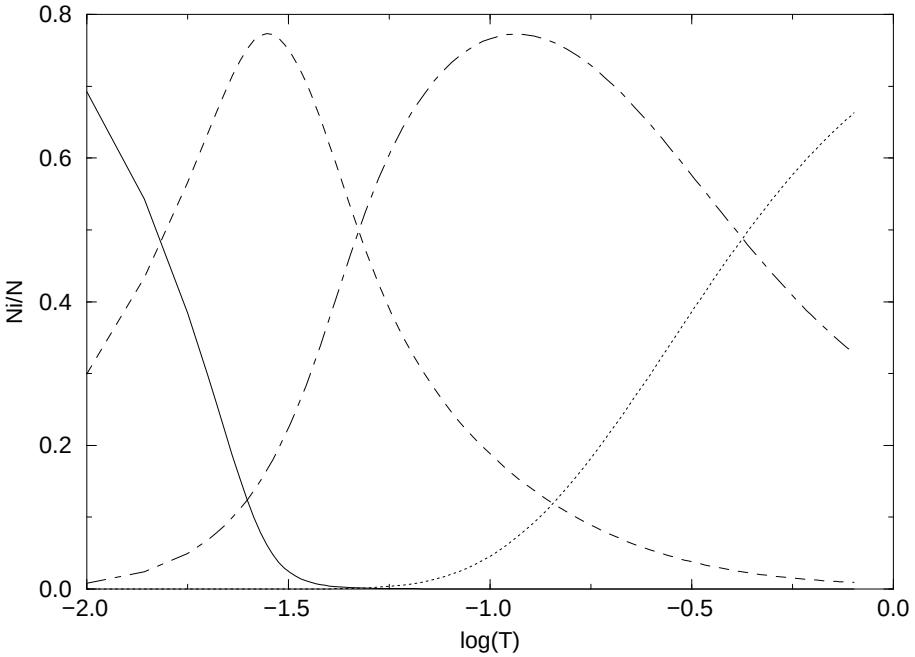

Figure 7. The logarithmic T scale is used for the three-step behaviour shown in figure 6. The same parameters as in figure 6 are used.

for $\eta_2, \eta_3 \ll 1$. For large N and $c_2 = 1$, we simply have

$$\frac{T_{2D}^*}{T_{2D}} = 1 + \frac{5}{8}\left(\frac{\kappa}{N\zeta(2)}\right)^{1/2} \log\left(\frac{N}{\kappa\zeta(2)}\right). \tag{60}$$

The one-dimensional crossover temperature T_{1D}^* has the same form as in the prolate shape potential case.

The conditions (A) and (B) in equation (38) give the constraints for anisotropy parameters for three-step behaviour to be observed:

$$\begin{aligned} \kappa &> \frac{N\zeta(2)}{(\log(2N))^2} \\ k_3 &> \frac{\zeta(3)}{\zeta(2)}\frac{N}{\log(2N)}. \end{aligned} \tag{61}$$

If $T_{2D} \ll T_{3D}$ holds, since it also implies $T_{2D} \ll \omega_1$, excitations along the first axis will be dynamically suppressed at $T < \omega_1$ making the system effectively two-dimensional before BEC sets in. Furthermore, if $T_{1D} \ll T_{2D}$ is also satisfied, BEC occurs in two steps, one at T_{2D} and the other at T_{1D}. In figure 6, the above senario of three-step dimensional reduction is numerically realized. Three-dimensionally excited modes dominant at higher temperature are dynamically suppressed at $T < \omega_1$, followed by two-step BEC. When the condensation into the ground state sets in, the effective dimension of the system is still two. From the form of critical temperatures in equations (44) and (53), we see that high anisotropy and the small number of atoms have similar consequences.

It is useful to see how the weak interaction effect modifies the above arguments†. The shift of the critical temperature due to the interaction effect is given in [33] as $\Delta T_{3D}^{\rm int}/T_{3D} \sim$

† We recover ordinary units in this discussion for quantitative comparison with other literature.

$aN^{1/6}/L$, where a is the s-wave scattering length, $L \equiv \sqrt{\hbar/m\Omega}$. The shift due to finite size is given in equation (57) as $\Delta T^*_{3D}/T_{3D} \sim (k_3/N)^{1/3}$. For a reasonable choice of parameters, $N = 5000$, $k_3 = 10$, $a/L = 0.001$, we obtain $\Delta T^{\rm int}_{3D}/T_{3D} \sim 0.003$ and $\Delta T^*_{3D}/T_{3D} \sim 0.13$. Thus the interaction effect is negligible compared to the finite size correction.

Comparing the zero-point energy in the most confining direction with the interaction energy, if $\omega_1 > n_0 U$, where n_0 is the ground state density and $U \equiv 4\pi\hbar^2 a/m$, the criteria for the system to behave as effectively two-dimensional is still given by $\omega_1 > T$. For the choice of value $n_0 U/k_B \sim 110$ (nK) for a sodium atom, this gives $\omega_1 > n_0 U \sim 10^4$ ($1\ {\rm s}^{-1}$). We should note that the collision effect even in such a case cannot be strictly two-dimensional [34]; for high energy atoms, the interaction vertex has the form of the three-dimensional one. Nevertheless, these effects will be still suppressed for $a \ll L_1$ and a small number of particles, whereas the finite size correction behaves as $\Delta T^*_{2D}/T_{2D} \sim (\kappa/N)^{1/2}$ and $\Delta T^*_{1D}/T_{1D} \sim 1/\log N$. Therefore, the effect of interaction on the particle number and the critical temperature remains small and the system is still expected to show the multistep behaviour under these conditions. At $T < \omega_1$, the most notable difference would be the absence of long-range order due to interactions in this effectively two-dimensional system. In this case, the system can show quasi-condensation, the condensation with the fluctuating phase at near T_{2D}. The true condensation with the constant phase will be acheived at lower temperature. One example of a quasi-two-dimensional system, a gas of spin-polarized hydrogen in liquid helium, is known to exhibit Kosterlitz–Thouless transition [35, 36]. Manifestation of the crossover from BEC to Kosterlitz–Thouless transition [37] during the multistep process is of particular interest to study. However, even in the presence of such a transition, we expect that the particle occupation number which is insensitive to the phase information will still behave similar to the ideal gas. The interaction contributions used above are calculated within the framework of the mean field theory. Thus we conclude, apart from the critical regime where the mean field theory fails, interactions do not essentially alter the multistep process for a small number of atoms in highly anisotropic traps.

From the arguments given in this section, the sum of most relevant terms in equation (54) around each crossover temperature will give the simple expression of the total number of atoms as

$$N = N_0 + N_1 + N_2 + N_3 \sim g_0(\mathrm{e}^{-\phi}) + \frac{g_1(\mathrm{e}^{-\phi})}{\eta_3} + \frac{g_2(\mathrm{e}^{-\phi})}{\eta_2\eta_3} + \frac{g_3(\mathrm{e}^{-\phi})}{\eta_1\eta_2\eta_3}. \tag{62}$$

Making use of the fact that ϕ varies as a nonvanishing function of the temperature for the finite system, we define $N_3(\lambda) \equiv g_3(\mathrm{e}^{\lambda\phi})/\eta_1\eta_2\eta_3$. The relation for the Bose function $\partial_\phi g_n(\mathrm{e}^{-\phi}) = -g_{n-1}(\mathrm{e}^{-\phi})$ [4] allows us to write

$$\begin{aligned} N_2(\lambda) &\equiv \frac{g_2(\mathrm{e}^{\lambda\phi})}{\eta_2\eta_3} = \frac{1}{x_1}\frac{\mathrm{d}N_3(\lambda)}{\mathrm{d}\lambda} \\ N_1(\lambda) &\equiv \frac{g_1(\mathrm{e}^{\lambda\phi})}{\eta_3} = \frac{1}{x_1x_2}\frac{\mathrm{d}^2N_3(\lambda)}{\mathrm{d}\lambda^2} \\ N_0(\lambda) &\equiv g_0(\mathrm{e}^{\lambda\phi}) = \frac{1}{x_1x_2x_3}\frac{\mathrm{d}^3N_3(\lambda)}{\mathrm{d}\lambda^3}. \end{aligned} \tag{63}$$

Thus the total number of atoms is given by

$$N = \frac{1}{x_1x_2x_3}\frac{\mathrm{d}^3N_3(-1)}{\mathrm{d}\lambda^3} + \frac{1}{x_1x_2}\frac{\mathrm{d}^2N_3(-1)}{\mathrm{d}\lambda^2} + \frac{1}{x_1}\frac{\mathrm{d}N_3(-1)}{\mathrm{d}\lambda} + N_3(-1). \tag{64}$$

At $T \sim T^*_{3D}$, $x_1 \sim 1$ and $x_2, x_3 \gg 1$, then we have

$$N \sim \frac{\mathrm{d}}{\mathrm{d}\lambda}N_3(-1) + N_3(-1). \tag{65}$$

At $T \sim T^*_{2D}$, $x_2 \sim 1$, $x_1 \ll 1$ and $x_3 \gg 1$, we have

$$N \sim \frac{\mathrm{d}}{\mathrm{d}\lambda} N_2(-1) + N_2(-1). \tag{66}$$

At $T \sim T^*_{1D}$, $x_3 \sim 1$ and $x_1, x_2 \ll 1$, we have

$$N \sim \frac{\mathrm{d}}{\mathrm{d}\lambda} N_1(-1) + N_1(-1). \tag{67}$$

These results suggest that each condensation fraction N_i behaves similarly as a function of the temperature in the neighbourhood of its characteristic temperature T^*_{iD}. We simply write this fact as $N_i(T) \sim F(T/T^*_{iD})$ for $i = 1, 2, 3$, where F is a function independent of i. It also implies that each component has a similar shape in the logarithmic T scale. The occupation number of each dimension is plotted in the logarithmic T scale in figure 7. Note that this derivation relies on the special property of the Bose function which determines the density of states of an ideal gas trapped in the harmonic potential. Whether the same result holds or not in other systems with different density of states is not obvious.

In conclusion, finite size effects on the BEC of an ideal gas in a strongly anisotropic trap give rise to various different types of multistep behaviour depending on the degree of anisotropy. In an isotropic trap, BEC into the ground state always begins while the system is effectively three-dimensional, i.e. $T_{3D} > \omega_1 = \omega_2 = \omega_3$. In an anisotropic trap, in addition to the BEC which may occur in multisteps, EIRD will also decrease in steps as the temperature is lowered. The combined effect of these leads to the appearant multistep behaviour. The existence of the intermediate condensation into one-dimensional space can be traced back to the logarithmic divergence of the one-dimensional occupation number in equation (36). This means that, when the trap is loosened in one direction, the particles tend to occupy quantum states along this direction with more likelihood than along other directions. Thus one-dimensionally excited modes in this direction will dominate multidimensional excitations spread in other directions ($N_1 \gg N_2, N_3$) and the thermodynamic behaviour of such a system is characterized by T_{1D} even though effective dimension of the system is still three. Note that the same mechanism is responsible for the *nonexistence* of BEC in one-dimensional harmonic trap in the ordinary thermodynamic limit. For the same reason, the intermediate condensation into two-dimensionally excited modes can be observed in a rectangular cavity [10, 24], where T_{2D} does not exist in the naive thermodynamic limit. Three-step BEC can only take place in such a system. Away from the thermodynamic limit, the temperature dependence of the chemical potential around T_{1D}, T_{2D} and T_{3D} causes similar crossover behaviours in condensation fractions N_1, N_2 and N_3 as a function of the reduced temperature.

Atom trap experiments probing the two-step BEC are realizable in Ioffe–Pritchard-type magnetic traps or in optical dipole traps [24]. A similar type of device can be used to study multistep behaviour discussed here, although it is difficult to achieve BEC in a maximally anisotropic trap with our current cooling technique. Further progress in a trapping device may be required. The basic mechanism of multistep dimensional crossovers discussed here can be applied to many other bosonic systems and should be amenable to future experimental verification. Quasi low-dimensional systems realized in the optical lattice or waveguide are a promising option for testing such processes [17,18]. Also of interest is the kinetics of multistep behaviour where the correlation length and the thermal de Broglie wavelength are related in a nontrivial manner. This is currently under investigation.

Acknowledgments

The author appreciated Professor B Hu for the hospitality of the Center for Nonlinear Studies at Hong Kong Baptist University during his visit from March to September 1998. He also thanks Professor B L Hu for various discussions, Professor J Weiner for useful comments, particularly of experimental relevance, and Dr K Kirsten for useful references.

Appendix A. Dynamical symmetry in anisotropic harmonic oscillator

It is known that dynamical symmetry of anisotropic harmonic oscillators has the reducible representation which can be written as the multiple of irreducible representation of $SU(3)$ symmetry, the symmetry of isotropic harmonic oscillators.

For a given $\lambda = (\lambda_1, \lambda_2, \lambda_3)$, we can define a set of many boson annihilators [38] as

$$A_i^\lambda = a_i^{k_i} \sqrt{\left[\frac{\hat{n}_i}{k_i}\right] \frac{(\hat{n}_i - k_i)!}{\hat{n}_i!}} \qquad \text{for} \quad i = 1, 2, 3 \tag{A1}$$

where $\hat{n}_i = a_i^\dagger a_i$ are boson number operators. Many boson annihilators and creators satisfy the following commutation relations:

$$[A_i^\lambda, A_j^{\lambda\dagger}] = \delta_{ij}. \tag{A2}$$

Rewriting Hamiltonian (4) as

$$H = \frac{\omega}{2} \sum_{i=1}^{3} \{A_i^\lambda, A_i^{\lambda\dagger}\} - \frac{1}{2} \sum_{i=1}^{3} \omega_i (k_i - 2\lambda_i - 1) \tag{A3}$$

the corresponding energy eigenvalue becomes

$$E_n = \omega(M + \tfrac{3}{2}) - \tfrac{1}{2} \sum_{i=1}^{3} \omega_i (k_i - 2\lambda_i - 1). \tag{A4}$$

This gives the alternative method to derive energy eigenvalues given in equation (6).

Thus the reducible representation (4) of the original Hamiltonian leads to the cluster of isotropic harmonic oscillators. With this decomposition, it is possible to understand the mechanism of condensation in anisotropic traps in terms of condensation in isotropic traps [39].

Appendix B. Mathematical formulae

By taking derivatives of

$$\sum_{M=0}^{\infty} \mathrm{e}^{-M\eta} = \frac{1}{1 - \mathrm{e}^{-\eta}} \tag{B1}$$

with respect to η on both sides, we obtain

$$\sum_{M=1}^{\infty} M\mathrm{e}^{-M\eta} = \frac{\mathrm{e}^{-\eta}}{(1 - \mathrm{e}^{-\eta})^2} \tag{B2}$$

and

$$\sum_{M=1}^{\infty} M^2\mathrm{e}^{-M\eta} = \frac{\mathrm{e}^{-\eta}(1 + \mathrm{e}^{-\eta})}{(1 - \mathrm{e}^{-\eta})^3}. \tag{B3}$$

For a small η, we have an expansion

$$\frac{\mathrm{e}^{-\eta}}{1-\mathrm{e}^{-\eta}} = \frac{\mathrm{e}^{-\eta/2}}{2\sinh(\eta/2)} = \frac{\mathrm{e}^{-\eta/2}}{\eta} - \frac{\eta \mathrm{e}^{-\eta/2}}{24} + \cdots. \tag{B4}$$

Similarly, we have

$$\frac{\mathrm{e}^{-k\eta}}{(1-\mathrm{e}^{-k\eta})(1-\mathrm{e}^{-\eta})} = \frac{\mathrm{e}^{-(k-1)\eta/2}}{k\eta^2} - \left(k+\frac{1}{k}\right)\frac{\mathrm{e}^{-(k-1)\eta/2}}{24} + \cdots \tag{B5}$$

and

$$\begin{aligned}\frac{\mathrm{e}^{-\eta_1}}{(1-\mathrm{e}^{-\eta_2})(1-\mathrm{e}^{-\eta_3})} &= \frac{\mathrm{e}^{-(\eta_1-\eta_2-\eta_3)/2}}{8\sinh(\eta_1/2)\sinh(\eta_2/2)\sinh(\eta_3/2)} \\ &= \frac{\mathrm{e}^{-(\eta_1-\eta_2-\eta_3)/2}}{\eta_1\eta_2\eta_3} - \frac{\mathrm{e}^{-(\eta_1-\eta_2-\eta_3)/2}}{24}\left(\frac{\eta_1^2+\eta_2^2+\eta_3^2}{\eta_1\eta_2\eta_3}\right) + \cdots.\end{aligned} \tag{B6}$$

From equation (B4),

$$\sum_{l=1}^{\infty}\frac{z^l\mathrm{e}^{-l\eta}}{1-\mathrm{e}^{-l\eta}} \sim \sum_{l=1}^{\infty}\frac{z^l\mathrm{e}^{-l\eta/2}}{l\eta} = -\frac{1}{\eta}\log(1-z\mathrm{e}^{-\eta/2}). \tag{B7}$$

References

[1] Bose S N 1924 *Z. Phys.* **26** 178
[2] Einstein A and Preus S B 1924 *Akad. Wiss.* **22** 261
[3] Huang K 1987 *Statistical Mechanics* (New York: Wiley)
[4] Pathria R K 1996 *Statistical Mechanics* (Oxford: Butterworth-Heinemann)
[5] Anderson M H, Ensher J R, Matthews M R, Wieman C E and Cornell E A 1995 *Science* **269** 198
[6] Davis K B, Mewes M-O, Andrews M R, van Druten N J, Durfee D S, Kurn D M and Ketterle W 1995 *Phys. Rev. Lett.* **75** 3969
[7] Mewes M-O, Andrews M R, van Druten N J, Kurn D M, Durfee D S and Ketterle W 1996 *Phys. Rev. Lett.* **77** 416
[8] Griffin A, Snoke D W and Stringari S (ed) 1995 *Bose–Einstein Condensation* (Cambridge: Cambridge University Press)
[9] Krueger D A 1968 *Phys. Rev.* **172** 211
[10] Sonin E A 1969 *Sov. Phys.–JETP* **29** 520
[11] Osborne M F M 1949 *Phys. Rev.* **76** 396
[12] Bagnato V and Kleppner D 1991 *Phys. Rev.* A **44** 7439
[13] Grossmann S and Holthaus M 1995 *Phys. Lett.* A **208** 188
[14] Kirsten K and Toms D J 1996 *Phys. Lett.* A **222** 148
Kirsten K and Toms D J 1996 *Phys. Rev.* A **54** 4188
Kirsten K and Toms D J 1999 *Phys. Rev.* E **59** 158
[15] Grossmann S and Holthaus M 1995 *Z. Naturf.* a **50** 921
[16] Ingold G and Lambrechet A 1998 *Eur. Phys. J.* D **1** 29
[17] Gauk H, Hartl M, Schneble D, Schnitzler H, Pfau T and Mlynek J 1998 *Phys. Rev. Lett.* **81** 5298
[18] Vuletic V, Kerman A J, Chin C and Chu S 1999 *Phys. Rev. Lett.* **82** 1406
[19] Fisher M E 1971 Critical phenomena *Proc. 51st Enrico Fermi Summer School (Varenna, Italy)* ed M S Green (New York: Academic)
[20] Barber M N and Fisher M E 1973 *Phys. Rev.* A **8** 1124
[21] Barber M N 1983 *Phase Transitions and Critical Phenomena* vol 8, ed C Domb and J L Lebowitz (New York: Academic)
[22] Hu B L and O'Connor D J 1984 *Phys. Rev.* D **30** 743
Hu B L and O'Connor D J 1987 *Phys. Rev.* D **36** 1701
[23] O'Connor D J, Stephens C R and Hu B L 1988 *Ann. Phys.* **190** 310
[24] van Druten N J and Ketterle W 1997 *Phys. Rev. Lett.* **79** 549
[25] Shiokawa K and Hu B L 1999 *Phys. Rev.* D **60** 105016
[26] Bagnato V, Pritchard D E and Kleppner D 1987 *Phys. Rev.* A **35** 4354

[27] Ensher J R, Jin D S, Matthews M R, Wieman C E and Cornell E A 1996 *Phys. Rev. Lett.* **77** 4984
[28] Haugerud H, Haugset T and Ravndal R 1997 *Phys. Lett.* A **225** 18
Haugerud H, Haugset T and Andersen O 1997 *Phys. Rev.* A **55** 2922
[29] Baym G and Pethick C 1996 *Phys. Rev. Lett.* **76** 6
[30] Chou T T, Yang C N and Yu L H 1996 *Phys. Rev.* A **53** 4257
[31] Gunton J D and Buckingham M J 1968 *Phys. Rev.* **166** 152
[32] Ketterle W and van Druten N J 1996 *Phys. Rev.* A **54** 656
[33] Georgini S, Pitaevskii L P and Stringani S 1996 *Phys. Rev.* A **54** R4633
[34] Kagan Yu, Svistunov B V and Shlyapnikov G V 1987 *Sov. Phys.–JETP* **66** 480
[35] Silvera I F 1995 *Bose–Einstein Condensation* ed A Griffin *et al* (Cambridge: Cambridge University Press)
[36] Safonov A I, Vasilyev S A, Yasnikov I S, Lukashevich I I and Jaakkola S 1998 *Phys. Rev. Lett.* **81** 4545
[37] Petrov D S, Holtzmann M and Shlyapnikov G V 1999 Bose–Einstein condensation in quasi 2d trapped gases *Preprint* cond-mat/9909344
[38] Brant R A and Greenberg O W 1968 *J. Math. Phys.* **10** 1168
[39] Nazarewicz W and Dobaczewski J 1992 *Phys. Rev. Lett.* **68** 154